

THESIS FOR THE DEGREE OF LICENTIATE OF ENGINEERING IN THERMO  
AND FLUID DYNAMICS

Turbulence-droplet interaction modelled by  
One-Dimensional-Turbulence

MARCO FISTLER

Department of Mechanics and Maritime Sciences  
CHALMERS UNIVERSITY OF TECHNOLOGY

Gothenburg, Sweden 2017

Turbulence-droplet interaction modelled by One-Dimensional-Turbulence  
MARCO FISTLER

© MARCO FISTLER, 2017

Thesis for the degree of Licentiate of Engineering 2017:13  
Department of Mechanics and Maritime Sciences  
Chalmers University of Technology  
SE-412 96 Gothenburg  
Sweden  
Telephone: +46 (0)31-772 1000

Chalmers Reproservice  
Gothenburg, Sweden 2017

Turbulence-droplet interaction modelled by One-Dimensional-Turbulence  
Thesis for the degree of Licentiate of Engineering in Thermo and Fluid Dynamics  
MARCO FISTLER  
Department of Mechanics and Maritime Sciences  
Chalmers University of Technology

## ABSTRACT

A stochastic model to study droplet/particle influence on the gas phase using the One-Dimensional-Turbulence model (ODT) is evaluated. To address one of the major problems for multiphase flow simulations, namely computational costs, the dimension-reduced model is used with the goal of predicting certain classes of these flows more efficiently. ODT is a stochastic model simulating turbulent flow evolution along a notional one-dimensional line of sight by applying instantaneous maps which represent the effect of individual turbulent eddies on property fields. A Lagrangian particle tracking method developed by Schmidt et al. [10] was modified and extended.

For validation purposes flow configurations of turbulent particle-laden round jet were simulated with the developed model. It could be shown that the model has the capability to capture the impact of varying Stokes numbers and also different particle loadings. This shows that turbulence modulation is possible to capture with the model and it can be used for investigations of turbulent-droplet interaction at parameter ranges which are not accessible by DNS or LES simulations.

Keywords: Turbulence, Droplets, Multiphase Flow, One Dimensional Turbulence(ODT)



## LIST OF PUBLICATIONS

This thesis is based on the work contained in the following publications:

- Publication A** M. Fistler, D. O. Lignell, A. Kerstein and M. Oevermann, "Numerical study of stochastic particle dispersion using One-Dimensional-Turbulence" in *ILASS-Americas 2017*.
- Publication B** M. Fistler, D. O. Lignell, A. Kerstein and M. Oevermann, "Numerical studies of turbulent particle-laden jets using spatial approach of one-dimensional turbulence" in *ILASS-Europe 2017*.



## ACKNOWLEDGEMENTS

Cooperation and interaction are the foundation of good research and a good life. That is why it is almost impossible to sit alone in your basement and contribute to the scientific field. I had the great opportunity to work with some genius and awesome personalities from all over the world. Here is not enough space to thank them all but I have to point out the most important ones which shaped my work and life during the licenciate period.

As the one who made it all possible in the first place and who is supporting me with all he can I want to thank Michael Oevermann. He was doing more than just supervising my work. Whenever I had an idea or issue he was available to discuss it, to encourage me and to guide me in the right direction. Without his network and knowledge this thesis wouldn't be as it is. I also want to thank Alan Kerstein for all his time he spent to explain me ODT and to make sure I am on the right track. Thanks for the hours we were discussing principles of statistics, physics and ODT. Another important person is David Lignell, who provided his code for me and had the patience to describe it to me in lots of skype calls. Even at my short research visit in Utah he dedicated all his available time to me and therefore I am very thankful for your amazing hospitality and to get to know you personally.

But there are people which makes you surviving at periods where deadlines are coming closer, codes are bugging and reports do not want to be written by itself. These are the people which you see every day. To all my dear colleagues at Chalmers, there are no words for describing my pleasure which I have working beside you. If it is just sitting together for lunch or drinking after work, I always felt lucky to know you. A special thanks goes to Jelmer who suffered from my amazing music taste and cheered me when I was frustrated. Thanks for all the controversial discussion and freaky moments.

Without the most important people in my life I would not have been able to come to Sweden. All my confidence and determination bases on the security I experienced from my parents and my brother. They supported all my crazy ideas and always gave me the feeling to be there if it goes wrong. I am so happy to have you. Last but not least, I want to thank Fiona for her love and her patience with me. I cannot and do not want to imagine who I would be without you.



# Contents

Abstract	i
List of publications	iii
Acknowledgements	v
<b>1 Introduction</b>	<b>1</b>
1.1 Sprays and HAoS . . . . .	1
1.2 CFD and ODT . . . . .	3
<b>2 Physical Fundamentals</b>	<b>5</b>
2.1 Turbulence . . . . .	5
2.2 Droplets and Particles . . . . .	8
2.2.1 Shape . . . . .	8
2.2.2 Equation of Motion . . . . .	8
2.2.3 Coupling effects . . . . .	11
<b>3 One-Dimensional-Turbulence</b>	<b>13</b>
3.1 Diffusive advancement . . . . .	13
3.2 Eddy events . . . . .	15
3.2.1 Triplet map . . . . .	15
3.2.2 Eddy sampling . . . . .	19
<b>4 Lagrangian Particle Model</b>	<b>21</b>
4.1 Particle motion during diffusive advancement . . . . .	21
4.2 Particle-eddy interaction model . . . . .	21
<b>5 Contribution to the Field</b>	<b>25</b>
5.1 Paper I . . . . .	25
5.2 Paper II . . . . .	25
<b>6 Future work</b>	<b>27</b>
References	29



# 1 Introduction

The combustion of liquid fuel accounts for around  $\sim 30\%$  of the total energy consumed globally [7]. The current big discussions about the electrification of cars aim almost exclusively at light-duty vehicle transportation. For heavy-duty vehicles, marine vessels and airplanes it cannot be foreseen when the technology will be advanced enough to replace their combustion propulsion systems. In the near future the freight and passenger market covered by these transportation systems will grow rapidly. The *International Energy Agency* expects till 2050, compared to 2009, twice the transport load covered by trucks, three-fold by ships and four-fold by airplanes [11]. The growth will result in an inevitable environmental impact, which can be relaxed by the improvement of the combustion systems towards efficiency increase and pollution reduction. The demand for improvements is also forced by emission legislations of the European Union and other governmental institutions. Therefore, emission reduction is a key priority of the industry and has achieved big steps in the last decades, especially towards NO<sub>x</sub> and soot emissions. Despite the economic power and effort the advancement of fuel injection systems, which mainly governs the combustion process, is still compromised by an incomplete understanding of the physical mechanisms.

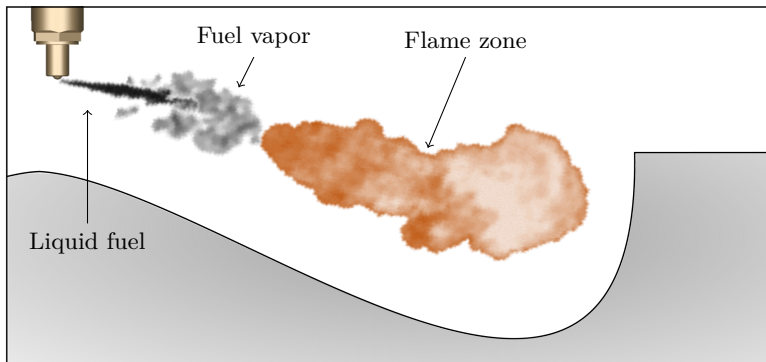


Figure 1.1: *Fuel injection in piston engine (Pictures of spray and flame by Chengjun Du)*

## 1.1 Sprays and HAoS

To tackle this issue eight European universities, including Chalmers University of Technology, joined by three industrial partners established a common project supported by the European Union and their Horizon 2020 initiative. Its goal is to develop a “Holistic Approach of Spray Injection through a generalized multi-phase framework”, short “HAoS”. In this scope each research facility is responsible for investigating a specific mechanism of the injected liquid jet configuration using experiments or simulations. Fig. 1.2 displays a schematic sketch of the spray regimes and their dominant physical mechanisms. It starts with the in-nozzle flow which is mainly governed by the pressure differences between nozzle

inlet and the in-nozzle geometry. Inside the nozzle *cavitation* can occur which leads to a partial reduction of the effective nozzle diameter. This is affecting flow and turbulence properties and is influencing the jet atomization regimes and mechanisms downstream. Behind the nozzle exit the liquid jet into the ambient air, which has a much lower pressure and density. In the first stage it is still a dense liquid core which first breaks up into larger ligaments and then into smaller droplets. The regime, where the first ligaments or droplets are shed from the liquid core, is called *primary atomization*. If these ligaments or droplets are getting smaller by breaking up further, it is called *secondary atomization*. In the last regime the now really small droplets are evaporating and form a fuel gas cloud around the spray, which can be ignited. When the spray becomes dilute, i.e. the volume ratio of liquid to gas phase is below  $10^{-2}$ , the interaction between droplets and turbulence becomes important. The so-called turbulence modulation introduced by droplets is, when transported downstream, effecting the fuel-air mixing process and so the flame regime. The investigation of this interaction and its governing mechanisms is the scope of this thesis.

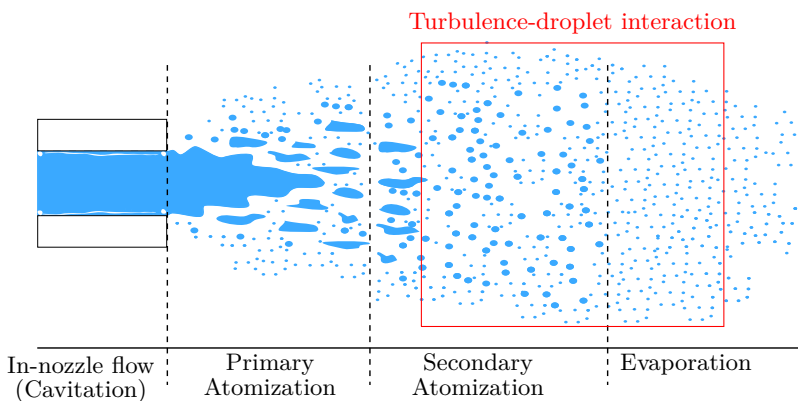


Figure 1.2: *Sketch of liquid spray regimes and its dominant mechanisms*

The effect of droplets or more general particles on the gas phase turbulence called turbulence modulation is of particular interest but the understanding of the phenomena is still lacking. Despite the fact that the first research in the field of dispersed two-phase flows can be traced back to the 17th century and research from Stevin and Newton, the biggest issue was ever since the understanding of turbulence itself [19]. Even with modern experimental equipment and high-performance computational flow simulations it is still challenging to capture the effects of the dispersed phase on the turbulent structures. In the last decades several research groups were investigating this field of interest and a brief summary can be read in the Ph.D. thesis of Poelma [19]. Different effects have been reported and in general it can be said that in some flow configurations the turbulence was enhanced and damped in others. The inertial effects of droplet size and mass compared to the one of the gas phase are mentioned to be the dominant parameter (more details in Chapter 2). Further studies are required to increase the knowledge of these effects and the sensitivity on this parameter.

## 1.2 CFD and ODT

CFD (computational fluid dynamics) proved to be a powerful tool to investigate dispersed two-phase flows and to acquire detailed flow information. However, many CFD approaches for these flow types have limited predictive capabilities or rely on many assumptions, which affects the accuracy and restricts their generality. Even with access to a high-performance computational infrastructure, direct numerical simulation (DNS) studies for particle-laden flow are still limited to academic cases and low particle numbers. On the other hand, the accuracy of large eddy simulations (LES) seems to be very sensitive to its parameters, especially on the subgrid-model, which is required to achieve a good turbulence prediction. In this study an alternative approach called One-Dimensional-Turbulence (ODT) is used, which was introduced in [13] and extended from several international research groups over the last two decades. ODT has demonstrated to predict topologically simple flows such as boundary layers and jets with large property gradients in one direction very well compared to DNS studies and experimental data. This stochastic model is used here to tackle one of the major problems for multiphase flow simulations, namely computational costs, with the goal to predict these types of flow more efficiently. By reducing the costs it will be possible to investigate parameter ranges with ODT which are unaccessible for DNS or LES. The final goal is to provide a subgrid-model for LES based on gathered data by ODT simulations. The numerical methodology of ODT and the Lagrangian particle model are described in Chapter 3 and 4, respectively.



## 2 Physical Fundamentals

In this chapter some features of turbulence and droplet evolution are summarized. Very detailed descriptions of these phenomena can be found in Pope [20] (turbulence) and Clift et al. [5] (droplets), but the important theoretical statements are summarized here for later consideration.

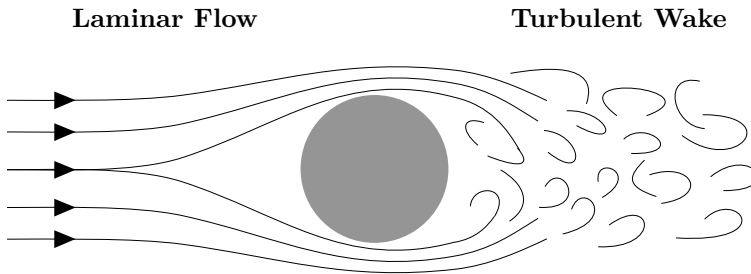


Figure 2.1: *Flow around a cylinder with a turbulent wake*

### 2.1 Turbulence

In a combustion engine (e.g. a gas turbine or a diesel engine) the fuel is injected into the combustion chamber by a high pressure drop, which results in a very high injection velocity. This is necessary to provide enough fuel in a short time frame and for a sufficient mixture of fuel and air. Due to the high velocity the liquid phase (fuel) is already turbulent when it exits the injector nozzle. But also the air flow around the liquid phase will become turbulent as a result of the high velocity gradients between the phases. These turbulent effects are causing deformations on the liquid phase and govern the break-up processes. The same phenomena occurs if turbulence interacts with smaller droplets till they are small enough to evaporate. But what is turbulence and how can we quantify it?

Turbulence is seen as a three-dimensional chaotic instability of flow properties caused by an increase of inertial forces relative to viscous damping. Above a critical value of the ratio between inertial and viscous forces a flow configuration is called turbulent (see Fig. 2.1). This knowledge goes back to the famous experiment of Osborne Reynolds (1883), where he found out that the occurrence of instabilities in a flow can be characterized by a single non-dimensional parameter. The parameter is called the Reynolds number and given as  $Re = \frac{L \cdot U}{\nu}$ , where  $L$  and  $U$  are characteristic integral length and velocity scales, respectively, describing the inertial effects.  $\nu$  is the kinematic viscosity. For different flow configurations different critical Reynolds numbers exist which are seen as a boundary between laminar and turbulent flow. For example, in case of a flow around a sphere the integral length scale is given by the sphere diameter and the characteristic velocity as the relative velocity between sphere and flow.

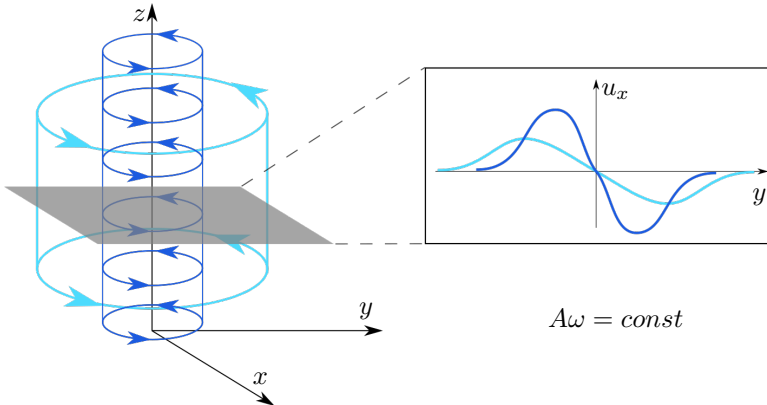


Figure 2.2: *Vortex stretching model by Bradshaw [4].*

The instantaneous turbulent movement is always rotational. Based on Helmholtz’s theorems for fluid motion in vortex filaments Bradshaw [4] described turbulence as a vortex stretching process. If we consider a Cartesian coordinate system  $(x,y,z)$  and a vortex filament along the  $z$ -axis, it is rotating in the  $xy$ -plane (Fig. 2.2). By stretching the vortex filament in  $z$  direction its cross-section will get smaller and due to the conservation of angular momentum, which is given as product of angular speed times cross-section, angular speed will increase. It means an extension in one direction decreases the length scale (cross-section or radius of the cross-section) and speeds up the velocity components in the other two directions. This in turn stretches other elements of fluid with vorticity components in these directions and so on [4], which results in a “cascade” of stretching processes with decreasing length scales. Summarized, the mechanism of vortex stretching shows that turbulence is distributing velocity fluctuations along all three components over all possible length scales. The range of length scales is limited by flow specific boundary conditions and viscosity, which is where the Reynolds number is referring to. The viscosity is smoothing large velocity gradients and determines the smallest possible length scale, called Kolmogorov scale, before kinetic energy dissipates into thermal internal energy.

Due to the appearance of instabilities in turbulent flows they are characterized by multiplexed three-dimensional, stochastic noise over a steady flow structure. Fig. 2.3 shows the axial velocity signal in a turbulent flow at a fixed position. Turbulence includes a randomness, which means its exact values are unpredictable. Hence, statistical tools are helpful treating the velocity values as a random process and representing its turbulent structure by statistical moments. Therefore, the velocity value is decomposed in an averaged *mean* component ( $\bar{u}$ ) and a randomly fluctuating *turbulent* part ( $u'$ ):  $u = \bar{u} + u'$ . Depending on your gathered data different averaging procedure can be applied, e.g. temporal, spatial or Ensemble average. Based on the first statistical moment, the second one (variance) can be determined with regard to the fluctuations. Due to the governing effect of turbulence the second moment is called turbulence intensity and given by the

*Root-(of-the-)mean-square* (RMS) values of the velocity fluctuations:

$$\sqrt{\overline{u'^2}}, \sqrt{\overline{v'^2}}, \sqrt{\overline{w'^2}}. \quad (2.1)$$

The above described decomposition is called *Reynolds decomposition*.

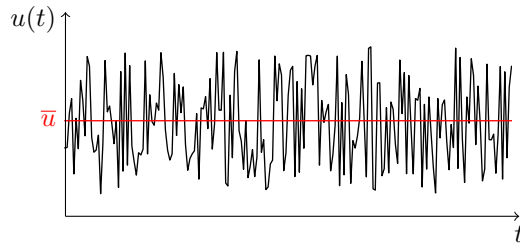


Figure 2.3: *Velocity signal over time in a turbulent flow*

Combining the concepts of vortex stretching and Reynolds decomposition turbulent flow contain a mean, turbulent and dissipative convection on a molecular level, where energy is transported from the mean (not necessarily) via the turbulent and subsequently to dissipation. These energy transport is called *energy cascade*.

## 2.2 Droplets and Particles

Investigating the behavior of multiple droplets in a turbulent flow it is important to understand first the fundamental behavior of a single droplet in a surrounding turbulent flow field. Therefore, it is necessary to assume common (simplified) properties for each droplet. In the following section the shape, equation of motion and coupling effects between both phases are discussed with its required assumptions and simplifications.

### 2.2.1 Shape

Initially, it is essential for the aerodynamic effects to define the shape of droplets. The range of droplet shapes is limited compared to solid particles due to its smooth surface caused by surface tension effects, but can change dynamically. Often they occur axisymmetric and under special circumstances spherical. In this study droplets are seen as spherical particles. The spherical shape can be assumed if inertial effects are considerably smaller than either inter-facial tension forces or the viscous forces of the surrounded phase. As droplets sizes in the far field region of a spray are relatively small these conditions are fulfilled. Hence, it leads to the rule-of-thumb to term droplets as spherical if the minor to major axis ratio is smaller than 10% [5]. Fig. 2.4 shows a regime diagram of droplet shapes depending on the non-slip Reynolds number ( $Re_p$ ) and the Eötvös number ( $Eo$ ), which are given as

$$Re_p = \frac{\rho_g |\vec{u}_p - \vec{u}_g| d_p}{\mu}, \quad Eo = \frac{g \Delta \rho d_p^2}{\sigma_p}. \quad (2.2)$$

The subscripts  $p$  and  $g$  are representing the dispersed (droplet) phase and the gas phase respectively.  $\rho$ ,  $\mu$  and  $\sigma_p$  are the density, viscosity and surface tension, respectively.  $g$  is the acceleration due to gravitation and  $d_p$  is the droplet diameter. In the two papers attached to the thesis the gravitational force was dominant and so the Eötvös number was the defining parameter. In future investigations closer to spray applications the effect of kinetic energy of the surrounding fluid will be more dominant. Here, a similar parameter exists, the so-called Weber number.

As we are investigating non-reacting flows at low temperatures in this study and the surface tension of diesel and other common fuels in sprays lies in a range of 20-30 mN/m for these conditions, the resulting  $Eo$  is below 10 for particles diameter in the order of  $10^{-5}$ m. The non-slip Reynolds number will not exceed 10 as well and therefore, we are in the regime of spherical droplets. From now on we will generalize droplets as spherical, rigid particles due to the facts that we do not consider break-ups or surface deformation.

### 2.2.2 Equation of Motion

Defining the behavior of a suspended, rigid sphere in a turbulent flow is in the scientific scope since centuries. It started with Stokes analytical solution for creeping flows ( $Re_p < 1$ ) (1851) and improvement suggestions by Oseen and Lamb (1910s). Using their basic ideas for relatively low Reynolds numbers several groups extended them resulting in the most

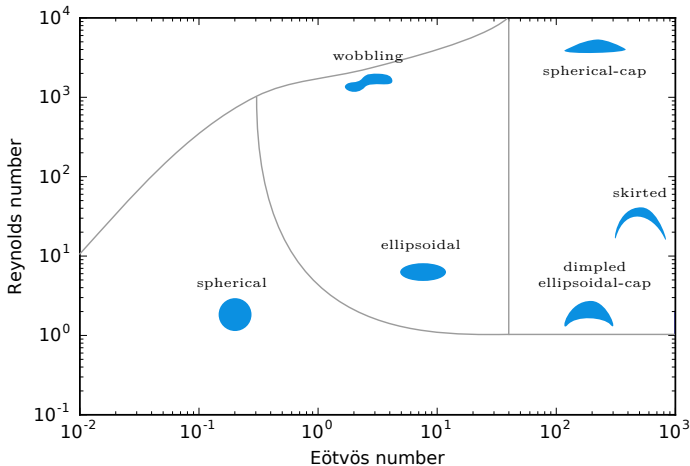


Figure 2.4: *Shape regimes for droplets (Adopted from Clift et al. [5])*

commonly used approximation for a sphere in an unsteady flow, which is the so-called Basset-Boussinesq-Oseen (BBO) equation. It summarizes all forces on a sphere in a non-stationary fluid and after several updates and corrections of Tchen (1947) and Maxey and Riley (1983) the current equation was derived as

$$m_p \frac{du_{p,i}}{dt} = F_G + F_P + F_{aM} + F_D + F_B \quad (2.3)$$

The equation consists of five terms on the right hand side which can be interpreted as gravitational ( $F_G$ ), pressure gradient ( $F_P$ ), added mass ( $F_{aM}$ ), Stokes drag ( $F_D$ ) and Basset ( $F_B$ ) forces. The two main assumptions, under which the equation is valid, are that the non-slip Reynolds number is smaller than unity and the particle size is smaller than the smallest structure of the flow (Kolmogorov scale [15]). Therefore, the particle can be seen as a point force located at the center of mass. Due to the assumptions stated above the flow is assumed to be symmetrical and uniform around the particle, so the BBO equations does not consider lift effects and the higher order terms of Eq. 2.3 can be neglected [19]. Also, if the density of the particle is assumed to be larger than the gas phase density, Eq. 2.3 leads to a simplified version only taking into account the dominating gravitational and drag forces, which leads to

$$m_p \frac{du_{p,i}}{dt} = m_p g_i - 3\pi d_p \eta (u_{p,i} - u_{g,i}). \quad (2.4)$$

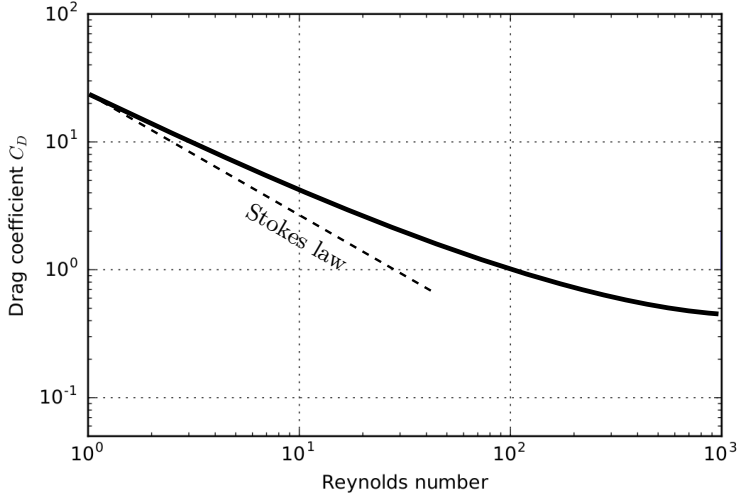


Figure 2.5: Drag coefficient of a sphere depending on non-slip Reynolds number (standard drag curve)[NASA GRC website]

The drag force term for an arbitrary shape is given as  $F_D = \frac{1}{2}\rho_g(u_{p,i} - u_{g,i}) \cdot A \cdot C_D$ , where  $A$  is the cross-section normal to the velocity component and  $C_D$  is the drag coefficient. Based on the first experiments by Stokes the drag coefficient were derived to  $C_D = \frac{24}{Re_p}$ , which leads to the second term on the right hand side of Eq. 2.4. By taking a look in the standard drag curve (Fig.2.5) we see a discrepancy for  $Re_p > 1$ . Schiller and Naumann [21] derived an empirical correction factor ( $f$ ) for non-slip Reynolds number smaller than 200. It is given as

$$f = (1 + 0.15Re_p^{0.687}). \quad (2.5)$$

Adding  $f$  to Eq. 2.4 and dividing by the mass of a spherical particle we get

$$\frac{du_{p,i}}{dt} = g_i - \frac{18\nu\rho_g}{d_p^2\rho_p} \cdot f(u_{p,i} - u_{g,i}). \quad (2.6)$$

Eq. 2.6 will be the starting point for the Lagrangian Particle model in the One-Dimensional Turbulence framework (Chapter 4).

As the factor  $\frac{18\nu\rho_g}{d_p^2\rho_p}$  has the dimensions  $s^{-1}$  it can be interpreted as the inverse of the time a particle needs to reach the velocity of the surrounding gas. It is the so-called Stokes time scale or particle relaxation time  $\tau_p$ . An important parameter for particle-turbulence interaction is the ratio of particle relaxation time ( $\tau_p$ ) to a characteristic flow time scale, the so-called Stokes number ( $St$ ). In this study the characteristic flow time scale will be the Kolmogorov time scale [15], which can be estimated by

$$\tau_\eta \approx \left( \frac{\nu L}{|u|^3} \right)^{1/2}, \quad (2.7)$$

where  $L$  is the integral length scale of the flow and  $u$  the velocity vector. This leads to

$$St = \frac{\tau_p}{\tau_\eta}. \quad (2.8)$$

As described in Chapter 1 the Stokes number represents the ratio of inertial forces of particle compared to the one of the gas phase.

### 2.2.3 Coupling effects

The interacting effects inside two-phase flows are classified in three groups based on the volume load, which are defined as a ratio of the volume occupied by the dispersed phase to the total volume plus gas phase (Elghobashi [8]),

$$\alpha = \frac{V_{dispersed}}{V_{tot}}. \quad (2.9)$$

In reality the two-phases are interacting with each other and additionally the particles can collide with each other. Capturing each interaction is high-costly for CFD solvers and therefore it is necessary to define regimes in which we can neglect some of the stated effects.

For the *one-way coupling* the momentum of the gas phase is coupled with the motion of the dispersed phase. The back-coupling effect is neglected. This is sufficient if the volume loading is in an order of  $10^{-6}$ - $10^{-5}$  depending on the density ratio. Above these values the energy and momentum transfer from the dispersed phase back to the gas phase increases significantly, which requires a so-called *two-way coupling*. Hence, both transport equations have to be solved in parallel and the governing gas phase equations contain a source term obeyed by the dispersed phase. If the volume loading increases further and the dispersed phase can not be characterized as diluted any more collision or hydrodynamic interactions can occur between the particles (*four-way coupling*). In the literature this regime starts from a volume loading of  $10^{-2}$ . However, more parameters are playing a key role here, i.e. relative velocity of the dispersed phase.

For spray applications the volume loading can be estimated by considering the spray dispersion as a cone geometry and taking the ratio of nozzle outlet area to the cross-section area further down stream (see Fig. 2.6). We assume that at the outlet the cross-section is only occupied by liquid fuel. To determine the distance from where we can assume a two-way coupling the spray cone angle  $\gamma$  is necessary to know. Based on the experimental data of Du [6] we assume a constant spray angle  $\gamma = 15^\circ$ . After using trigonometric relations and considering a very small axial distance  $\Delta x$  the volume loading is assumed as,

$$\alpha = \frac{V}{V'} = \frac{A\Delta x}{A'\Delta x} = \frac{\pi 4 D^2}{4 \pi D'^2} = \frac{D^2}{(D + 2\cos(\gamma)L)^2}. \quad (2.10)$$

Solving Eq. 2.10 for  $L$  gives,

$$L = \frac{D}{2\cos(\gamma)} \left( \frac{1}{\sqrt{\alpha}} - 1 \right). \quad (2.11)$$

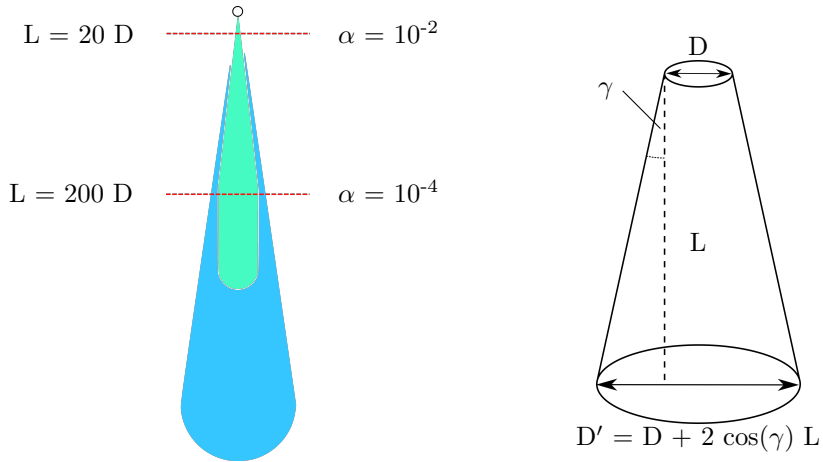


Figure 2.6: *Determination of volume loading in spray. a) shows a representation of liquid (green) and vapor (blue) phase of a spray (adopted from Du [6]) and the regime boundaries for two- and four-way coupling. b) shows a sketch to determine the volume loading  $\alpha$  by weighting the inlet area ( $A = \frac{\pi}{4} D^2$ ) to the area downstream depending ( $A' = \frac{\pi}{4} D'^2$ ) on spray cone angle  $\gamma$ .*

Here, the two-way coupling approach is valid after a distance of  $\sim 20D$  using the regime boundary  $\alpha = 10^{-2}$ . As the scope of this thesis is the area after the atomization regimes this assumption is reasonable and collision effects can be neglected.

Due to the developing steps of the Lagrangian tracking method the first study were made assuming a one-way coupling effect. For tracking a single particle this assumption is sufficient. The following studies focused on the two-way coupling approach, as the mass loadings are in the range 0.5 till 1 corresponding to volume loading from  $2 \cdot 10^{-4}$  -  $4 \cdot 10^{-4}$ .

### 3 One-Dimensional-Turbulence

This section describes the concept of the ODT model in the spatial-cylindrical framework, which is used to simulate the carrier gas phase. ODT is a numerical method to simulate realizations of turbulent flows using a stochastic model to capture the turbulent cascade along a one-dimensional line, which is usually oriented in the direction of the largest expected velocity gradient. The spatial-cylindrical domain can be seen as a radial line representing a slice of an axisymmetric phenomena evolving in an additional spatial dimension, which can be interpreted as a representation of a 3D unsteady flow field (Fig. 3.1). In the cylindrical coordinate system  $r, x$  and  $\theta$  are representing the radial, stream-wise and angular direction, respectively, whereas the latter will not be used due to a pre-assumed axisymmetry. Two main mechanism govern the ODT simulation, which are a diffusive flow advancement and a random sequence of eddy events to capture the impact of turbulence along the one-dimensional domain.

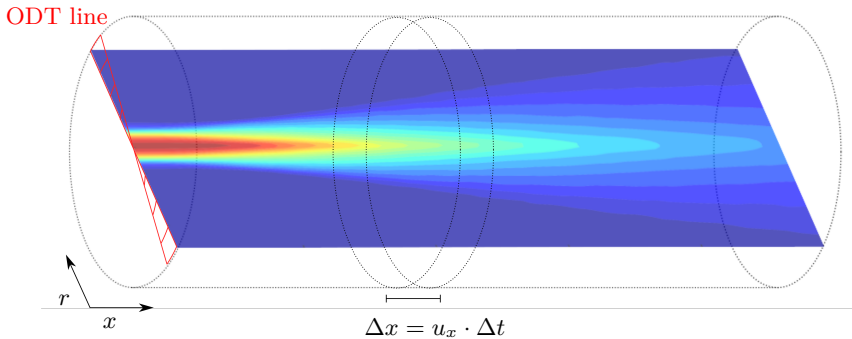


Figure 3.1: *ODT domain in a cylindrical coordinate system evolving in spatial direction  $\Delta x$ .*

#### 3.1 Diffusive advancement

Deriving the governing equations of an arbitrary quantity  $\phi$  for a control volume (seen in Fig. 3.2) we start with the Reynolds transport theorem (RTT) advanced in time  $t$ :

$$\frac{d}{dt} \int_{\Omega} \rho \phi dV = \frac{\partial}{\partial t} \int_{\Omega} \rho \phi dV + \int_{\partial\Omega} \rho \phi v_r \cdot n dS, \quad (3.1)$$

where  $\Omega$  is the control volume and  $\partial\Omega$  its boundary surface. The relative velocity between neighbour cells and control volume boundaries is represented by  $v_r$ . If we consider a strictly-positive stream-wise velocity, the temporal evolution can be transformed into a

spatial evolution by using the local stream-wise velocity  $u_x$ ,  $dt = \frac{dx}{u_x}$ . The transformed RTT is given as

$$\frac{d}{dx} \int_{\Omega} \rho u_x \phi dV = \frac{\partial}{\partial x} \int_{\Omega} \rho u_x \phi dV + \int_{\partial\Omega} \rho \phi v_r \cdot ndS. \quad (3.2)$$

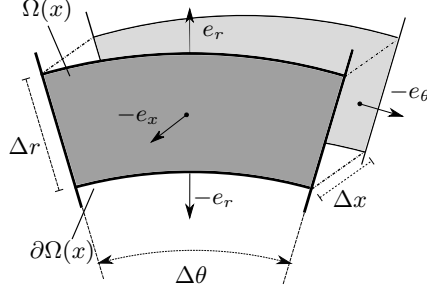


Figure 3.2: Sketch of control volume  $\Omega$ .  $e_i$  is a unit vector of the  $i$ -th direction.

Before deriving the governing equations for mass and momentum it is important to determine the control volume and its boundary surface on a cylindrical ODT line. The volume of a cylinder segment with the inner radius  $r_0$ , an outer radius  $r_1$ , an angle  $\theta$  and a length  $L$  is defined as  $V = \frac{\theta}{2} L (r_1^2 - r_0^2)$ . Its boundary surface is given by the two flat surfaces east  $e$  and west  $w$  and the two convex surfaces north  $n$  and south  $s$ . The area of the flat surface is given by  $A_{e,w} = \Delta r \cdot L$ , where  $\Delta r = r_1 - r_0$ , and the convex surface area as  $A_{n,s} = \theta r \cdot L$ . As we assume an axisymmetric flow configuration, which means an independence of the angular direction and velocity, the angle  $\theta$  is arbitrary and set to be 1 for simplicity. Additionally, a unit length  $L$  is assumed. This leads to the following definitions of control volume and convex surface

$$V = \frac{1}{2} (r_1^2 - r_0^2) \quad (3.3)$$

$$A_{n,s} = r. \quad (3.4)$$

To derive the mass balance equation the modified RTT (Eq. 3.2) is considered taken with  $\phi = 1$ . As no source terms are considered in the control volume  $\Omega$  during spatial step  $dx$ , the first term on the right hand side is zero and the general mass balance is given as

$$\frac{d}{dx} \int_{\Omega} \rho u_x dV = \int_{\partial\Omega} \rho v_r \cdot ndS + d\rho. \quad (3.5)$$

Here,  $d\rho$  is the mass change during an eddy event, which has just an effect in the eddy region and is zero outside of it. For an axisymmetric flow it is assumed that the angular velocity component is zero and therefore no fluxes exist over the planar surfaces east and west. After rearranging terms the mass balance in a given grid cell is given as

$$\frac{d\rho V}{dx} = \frac{1}{u_x} \left( \rho u_{r,s} A_s - \rho u_{r,n} A_n + d\rho \right). \quad (3.6)$$

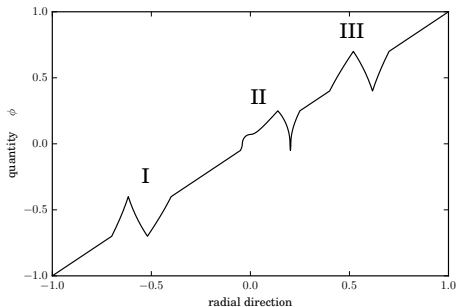


Figure 3.3: *Examples for applying a cylindrical triplet map to a linear profile of quantity  $\phi$ . I:  $r_0, r_0 + l < 0$ , II:  $r_0 < 0, r_0 + l > 0$ , III:  $r_0, r_0 + l > 0$ , where  $r_0$  and  $l$  are eddy position and length, respectively.*

For the momentum balance Eq. 3.2 is used with  $\phi = u_i$  and  $v_r = 0$ , where  $u_i$  represents the  $i$ -th velocity component. As the pressure term is neglected in this flow configuration and only viscous stress terms are considered, the momentum balance equation is given as

$$\frac{d}{dx} \int_{\Omega} \rho u_x u_i dV = \int_{\partial\Omega} \mu \tau_i dS + d_{\rho u_i} + S_{p,i}, \quad (3.7)$$

where  $\tau_i = \frac{\partial u_i}{\partial r}$  is the stress tensor,  $S_{p,i}$  represents the momentum exchange between dispersed and gas phase and  $d_{\rho u_i}$  is the momentum change during an eddy event. The latter is only non-zero in the eddy region. By rearranging and integrating over the cell volume and surfaces the momentum balance for a given grid cell is defined as

$$\frac{du_i}{dx} = \frac{1}{\rho u_x V} \left( \tau_{i,s} A_s - \tau_{i,n} A_n + d_{\rho U_i} + S_{p,i} \right). \quad (3.8)$$

Eq. 3.6 and 3.8 are the set of equation, which governs the diffusion and non-advective advancement, i.e. momentum exchange between phases, of the ODT line.

## 3.2 Eddy events

In ODT simulations turbulence, which can be seen as a three-dimensional vortex stretching process, is modeled through eddy events. These result in remapping the flow quantity profiles over a sampled eddy region. This model consists of two key components, the mapping method, which is called triplet map, and a model to define the rate of eddy events [13].

### 3.2.1 Triplet map

The original triplet map function, as introduced in Kerstein [13], used a planar coordinate system. Here, the original profile would be compressed by a factor of three over the eddy

region and three copies are filled in. To ensure continuity of the profile the second copy in the middle is inverted. In planar ODT the cell sizes depend only on the length in ODT line direction. However, in a cylindrical framework it depends on the square of the length due to the conservation requirements of mass, momentum and energy. As a result, in cylindrical coordinates the mapping process compresses the profiles with respect to the square of the length, which leads to the following inverse mapping function for a post-mapping position  $r_0$ , which is here  $r_0 \geq 0$ :

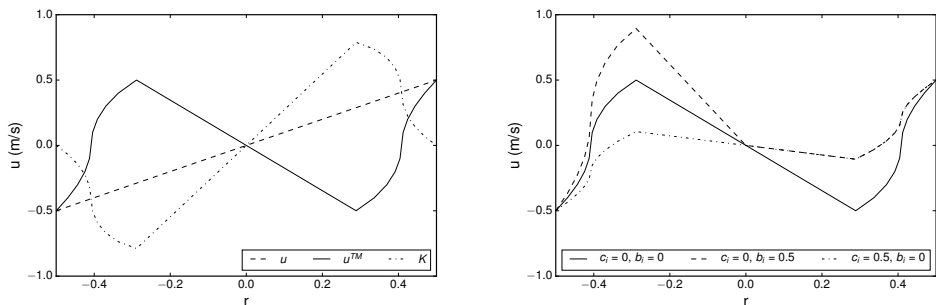
$$f(r) = r_0 + \begin{cases} \sqrt{9(r-r_0)^2} & \text{if } r \in [r_0, r_0 + \frac{l}{3}] \\ 2l - \sqrt{9(r-r_0)^2} & \text{if } r \in [r_0 + \frac{l}{3}, r_0 + \frac{2l}{3}] \\ \sqrt{9(r-r_0)^2} - 2l & \text{if } r \in [r_0 + \frac{2l}{3}, r_0 + l] \\ r - r_0 & \text{otherwise.} \end{cases} \quad (3.9)$$

For the case  $r_0 < 0$  the algebraic signs have to be adjusted in consideration of the possibility that  $r_0 + l$  is greater or smaller zero. Examples for the cylindrical triplet map are illustrated in Fig. 3.3.

An essential part of turbulence is the phenomena of return-to-isotropy, which requires a re-distribution of energy among the velocity components. This phenomena is modeled by introducing kernel transformations to the mapping function, which gives a profile transformation

$$u_i(r) \rightarrow u_i^{\text{TM}}(r) + c_i K(r) + b_i J(r), \quad (3.10)$$

where  $u_i$  is the velocity in  $i$ -th direction before and  $u_i^{\text{TM}}$  after the mapping process, respectively. The Kernel  $K(r)$  is defined as the fluid displacement profile under the triplet map and integrates to zero over the eddy region.  $J(r)$  is the absolute of  $K(r)$  and ensures momentum transfer if its kernel coefficient  $b_i$  is non-zero.  $c_i$  defines the kernel amplitude of  $K(r)$  and is mainly responsible for energy transfer (Fig. 3.4a and 3.4b). Thus, both kernels are important in the case of particle-gas phase coupling.



(a) Triplet map and its kernel function  $K$

(b) Influence of kernel function

Figure 3.4: Triplet map and the influence of its kernel functions

For the momentum flux conservation it is required that

$$\int_{r_0}^{r_0+l} \dot{\rho} u_i r dr = \int_{r_0}^{r_0+l} \dot{\rho} (u_i^{\text{TM}} + c_i K + b_i J) r dr + S_{p,i}, \quad (3.11)$$

where  $u_i$  is the velocity in  $i$ -th direction before and  $u_i^{\text{TM}}$  after the mapping process, respectively.  $\dot{\rho}$  is the mass flux in stream wise direction.  $S_{p,i}$  represents the sum of momentum penalties caused by particles

$$S_{p,i} = \sum_j^{n_p} \dot{m}_j (u_{j,i}^{\text{PEI}} - u_{j,i}^0), \quad (3.12)$$

where  $\dot{m}_j$  represents the stream-wise mass flux of the  $j$ -th particle.  $u_{j,i}^{\text{PEI}}$  and  $u_{j,i}^0$  determine the particle velocity component  $i$  after and before particle-eddy interaction, respectively. Due to the conservation of momentum flux during triplet mapping, which implies  $\int \dot{\rho} u_i r dr = \int \dot{\rho} u_i^{\text{TM}} r dr$ , it gives

$$b_i = \frac{-(S_{p,i} + c_i \int \dot{\rho} K r dr)}{\int \dot{\rho} J r dr} = -(M + c_i D). \quad (3.13)$$

For simplification  $M$  and  $D$  are used representing  $\frac{S_{p,i}}{\int \dot{\rho} J r dr}$  and  $\frac{\int \dot{\rho} K r dr}{\int \dot{\rho} J r dr}$ , respectively. Similar to the momentum flux conservation, the energy flux conservation is used to define  $c_i$ . As a result of the energy flux balance it is required that

$$\Delta E_i = \frac{1}{2} \int \dot{\rho} (u_i^{\text{TM}} + c_i K + b_i J)^2 r dr - \frac{1}{2} \int \dot{\rho} u_i^2 r dr. \quad (3.14)$$

Due to energy flux conservation during triplet mapping, which means  $\int \dot{\rho} u_i^2 r dr = \int \dot{\rho} (u_i^{\text{TM}})^2 r dr$ , it follows

$$\Delta E_i = \frac{1}{2} \int \dot{\rho} (2c_i u_i^{\text{TM}} K + 2b_i u_i^{\text{TM}} J + 2c_i b_i K J + c_i^2 K^2 + b_i^2 J^2) r dr. \quad (3.15)$$

Reordering with respect to  $c_i$  and inserting Eq. 3.13 for  $b_i$  yields

$$\begin{aligned} \Delta E_i &= c_i^2 \left( \frac{1}{2} \int \dot{\rho} K^2 r dr - D \int \dot{\rho} K J r dr + \frac{1}{2} D^2 \int \dot{\rho} J^2 r dr \right) \\ &\quad + c_i \left( \int \dot{\rho} u_i^{\text{TM}} K r dr - M \int \dot{\rho} K J r dr + MD \int \dot{\rho} J^2 r dr - D \int \dot{\rho} u_i^{\text{TM}} J r dr \right) \\ &\quad + \frac{1}{2} M^2 \int \dot{\rho} J^2 r dr - M \int \dot{\rho} u_i^{\text{TM}} J r dr. \end{aligned} \quad (3.16)$$

This can be written as

$$\Delta E_i = c_i^2 A + c_i B_i + C_i, \quad (3.17)$$

with

$$\begin{aligned}
A &= \frac{1}{2} \int \dot{\rho} K^2 r \, dr - D \int \dot{\rho} K J r \, dr + \frac{1}{2} D^2 \int \dot{\rho} J^2 r \, dr \\
B_i &= \int \dot{\rho} u_i^{\text{TM}} K r \, dr - M \int \dot{\rho} K J r \, dr + MD \int \dot{\rho} J^2 r \, dr - D \int \dot{\rho} u_i^{\text{TM}} J r \, dr \\
C_i &= \frac{1}{2} M^2 \int \dot{\rho} J^2 r \, dr - M \int \dot{\rho} u_i^{\text{TM}} J r \, dr.
\end{aligned} \tag{3.18}$$

Solved for  $c_i$  we get

$$c_i = \frac{1}{2 \cdot A} \left( -B_i + \text{sign}(B_i) \cdot \sqrt{B_i^2 - 4A(C_i - \Delta E_i)} \right). \tag{3.19}$$

$\Delta E_i$  governs the re-distribution of energy among velocity components and the loss and gain of energy from the particle phase. For the re-distribution the maximum available energy  $Q_i$  to subtract has to be determined ( $\frac{\partial \Delta E_i}{\partial c_i} = 0$ ), which is valid for:

$$c_i = -\frac{B_i}{2A}. \tag{3.20}$$

Inserted in Eq. 3.17 it gives

$$-\Delta E_i|_{\text{max}} = Q_i = \frac{B_i^2}{4A} - C_i. \tag{3.21}$$

Including the particle energy transfer during an eddy event,  $\Delta E_i$  is defined as:

$$\Delta E_i = \alpha \left[ \frac{Q_j - S_{\text{pE},j}}{2} + \frac{Q_k - S_{\text{pE},k}}{2} - Q_i \right] + (\alpha - 1) S_{\text{pE},i}. \tag{3.22}$$

$S_{\text{pE},i}$  represents the sum of energy penalties caused by particles

$$S_{\text{pE},i} = \frac{1}{2} \sum_j^{n_p} \dot{m}_j \left( (u_{j,i}^{\text{PEI}})^2 - (u_{j,i}^0)^2 \right). \tag{3.23}$$

The resulting kinetic energy of the sampled region, given by  $E_{\text{kin}} = \sum_i Q_i - S_{\text{pE},i}$ , is used to determine the eddy timescale  $t_e(l, r_0)$  and so to define the eddy event. Based on the scaling assumption for kinetic energy  $E \sim \frac{\rho l^3}{2t_e^2}$ , the eddy time scale is modeled as

$$\frac{1}{t_e} = C \sqrt{\frac{2KK}{\rho_{KK} l^2 V} (E_{\text{kin}} - Z E_{\text{vp}})}. \tag{3.24}$$

The viscous penalty energy is given as  $E_{\text{vp}} = \frac{\mu^2}{2\rho l}$ .  $C$  is the adjustable eddy rate parameter and scales the overall eddy event frequency.  $V$  is the volume of the eddy region.  $Z$  is the viscous penalty parameter, which suppresses unphysical small eddies. Also for large

eddies an equivalent procedure exists with a parameter noted as  $Z_{LES}$ .  $KK$  and  $\rho_{KK}$  are given by the following volume integrals over the eddy region:

$$KK = \int_V K(r)dV, \quad (3.25)$$

$$\rho_{KK} = \int_V \rho K(r)dV. \quad (3.26)$$

In the spatial version of ODT the eddy time  $t_e$  is multiplied by the favre-averaged velocity  $\tilde{u}$  over the eddy region to be transformed in a spatial dimension  $x_e$ . It can be interpreted as the way an eddy would need to develop the triplet map on the profile.

### 3.2.2 Eddy sampling

As a next step it is important to define the rate of eddy events  $\lambda$ , which is assumed to be depended on the eddy origin and length  $(r_0, l)$  and so on the current line state. This rate is modeled by using dimensional arguments, which are leading to

$$\lambda = \frac{1}{x_e l^2}. \quad (3.27)$$

The rate  $\lambda$  is the rate of eddies of length  $l$  in ODT-line and length  $x_e$  in stream-wise direction. Its integral over both quantities defines the rate of all eddies  $\Lambda$ . With both rates we can construct an instantaneous joint probability density function (PDF) of eddy size and location, which is given as

$$P(r_0, l) = \frac{\lambda(r_0, l)}{\int \int \lambda(r_0, l) dr_0 dl} = \frac{\lambda}{\Lambda}. \quad (3.28)$$

We assume that the occurrence of eddies of a certain size follows a Poisson process in space with a mean rate  $\Lambda$ , i.e.  $P(\Delta x) = \Lambda \exp(-\Lambda \Delta x)$ . Technically this is solved by oversampling, i.e. generation of candidate eddies at a much higher rate than requested, and thinning of the Poisson process with an acceptance-rejection method. For details we refer to [16].



# 4 Lagrangian Particle Model

In this chapter the particulate phase model is described which is modeled in a Lagrangian setting. The model consists of two parts corresponding to the two parts of the gas phase. The first part is for the diffusive advancement of particles and the second part for the instantaneous eddy events, which impose an instantaneous behaviour of the particulate phase.

## 4.1 Particle motion during diffusive advancement

The particulate phase is modelled in a Lagrangian way where individual particles are tracked following Newton's second law of motion. Here we consider the assumptions stated in Chapter 2. The set of equations governing the particle motion are:

$$\begin{aligned}\frac{du_{p,i}}{dt} &= -\frac{u_{p,i} - u_{g,i}}{\tau_p} f + g_i, \\ \frac{dr_p}{dt} &= u_{p,r}.\end{aligned}\tag{4.1}$$

The subscripts  $p$  and  $g$  represent the particle and the gas phase, respectively, and  $g_i$  is the  $i$ -th component of the gravity acceleration vector. The particle response time,  $\tau_p = \rho_p d_p^2 / 18\mu$  based on Stokes flow, is given here with consideration of mass  $m_p$  and density  $\rho_p$  of the particle and the fluid viscosity  $\mu$ . The factor  $f$  is defined as

$$f = 1 + 0.15Re_p^{0.687}.\tag{4.2}$$

The drag law (4.1) is solved by a first-order Euler method. As the ODT line evolves in spatial dimension ( $\Delta x$ ) this step has to be transformed to a temporal step with corresponding time step  $\Delta t$ . It means that each particle has its own time history and is time-independent of the ODT line. Therefore, a constant particle velocity over  $\Delta x$  is assumed, which yields to

$$\Delta t = \frac{\Delta x}{u_{p,x}}.\tag{4.3}$$

Again, we assume a strictly positive velocity  $u_x > 0$ .

## 4.2 Particle-eddy interaction model

The particle-eddy interaction (PEI) model is defined as the only effect of particle phase motion in ODT line-direction and so the relative velocity  $u_{p,r} - u_{g,r}$  in this direction for the drag law (Eq. 4.1) is zero. The PEI model in this study was developed by Schmidt et al. [22,23] as a so-called instantaneous PEI model (noted as *type-I*) and governs the lateral displacement due to an eddy event. Each particle obeys the model if they are located in the sampled eddy region. The main model assumption is that the eddy length scale  $x_e$ , transformed after Eq. 3.24, defines the distance an eddy needs to create the remapped

profile. That means before an eddy event the particle motion in (4.1) is integrated over the eddy time without a ODT-line velocity, which has to be corrected to account for a finite time a particle needs to cross an eddy of size  $x_e$ .

Therefore, the analytical solution for the drag law in ODT line-direction is used, which is given as

$$\begin{aligned} r_p &= r_{p0} + v_g t + \tau_p g_r t - \tau_p (\tau_p g_r + v_g - v_{p0}) (1 - e^{-t/\tau_p}), \\ v_p &= v_g + \tau_p g_r - (\tau_p g_r + v_g - v_{p0,i}) e^{-t/\tau_p}. \end{aligned} \quad (4.4)$$

where  $v_{p0}$  and  $r_{p0,i}$  are the initial particle velocity and location, respectively.  $\tau_p$  includes here the correction factor  $f$  (Eq. 4.2). As during the diffusive advancement the relative velocity in ODT line direction was assumed to be zero and with a new defined gas velocity for the PEI, so-called eddy velocity, the resulting correction over the time integral  $t_{pei}$  are

$$\begin{aligned} \Delta r_p &= v_g t_{pei} - v_g \tau_p (1 - e^{-t_{pei}/\tau_p}), \\ \Delta v_p &= v_g (1 - e^{-t_{pei}/\tau_p}), \end{aligned} \quad (4.5)$$

and the post-PEI location and velocity are  $r_p = r_{p0} + \Delta r_p$  and  $v_p = v_{p0} + \Delta v_p$ , respectively.

Now, it is required to define an eddy velocity in lateral direction  $v_e$  and an interaction time  $t_{pei}$ , which determines the time interval in Eq. 4.1, to correct the integration over the time interval  $t_{pei}$ . Determining the eddy velocity  $v_e$  during the eddy event, the concept of the displacement of a mass-less tracer particle governed by the mapping method (Eq. 3.9) is used. The triplet map provides three possible tracer particle positions and a unique position is sampled randomly with a uniform distribution from those three possible ones. The final displacement  $\Delta R_{TM}$ , see Fig. 4.1, divided by the eddy time scale  $t_e = x_e/u_p$  defines the gas velocity during the PEI.

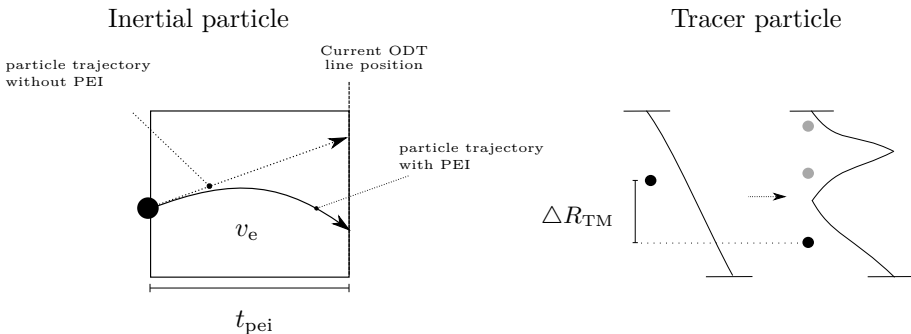


Figure 4.1: Example of re-integration of drag law (Eq. 4.1) over particle-eddy interaction time  $t_{pei}$ . Eddy velocity  $v_e$  is defined as the tracer particle displacement  $\Delta R_{TM}$  by the triplet map divided by the eddy time scale  $t_e = x_e/u_p$ . For the displacement one (black circle) of three possible positions (grey circles) is chosen randomly.

As a next step the integral time scale has to be determined and therefore a so-called eddy box is introduced with the dimensions  $[l \times l \times \beta_p x_e]$ , where  $\beta_p$  is a model parameter. The PEI integration time  $t_{\text{pei}}$  is given as the time the particle needs to exit the box. Therefore, the analytical solution (Eq. 4.4) is used again to compute the exit time in each direction. For the non-radial eddy velocity components the local gas velocity at the particle position is used. The minimum of the resulting exit times defines the particle-eddy interaction time  $t_{\text{pei}}$ .

Gas phase

Particle phase

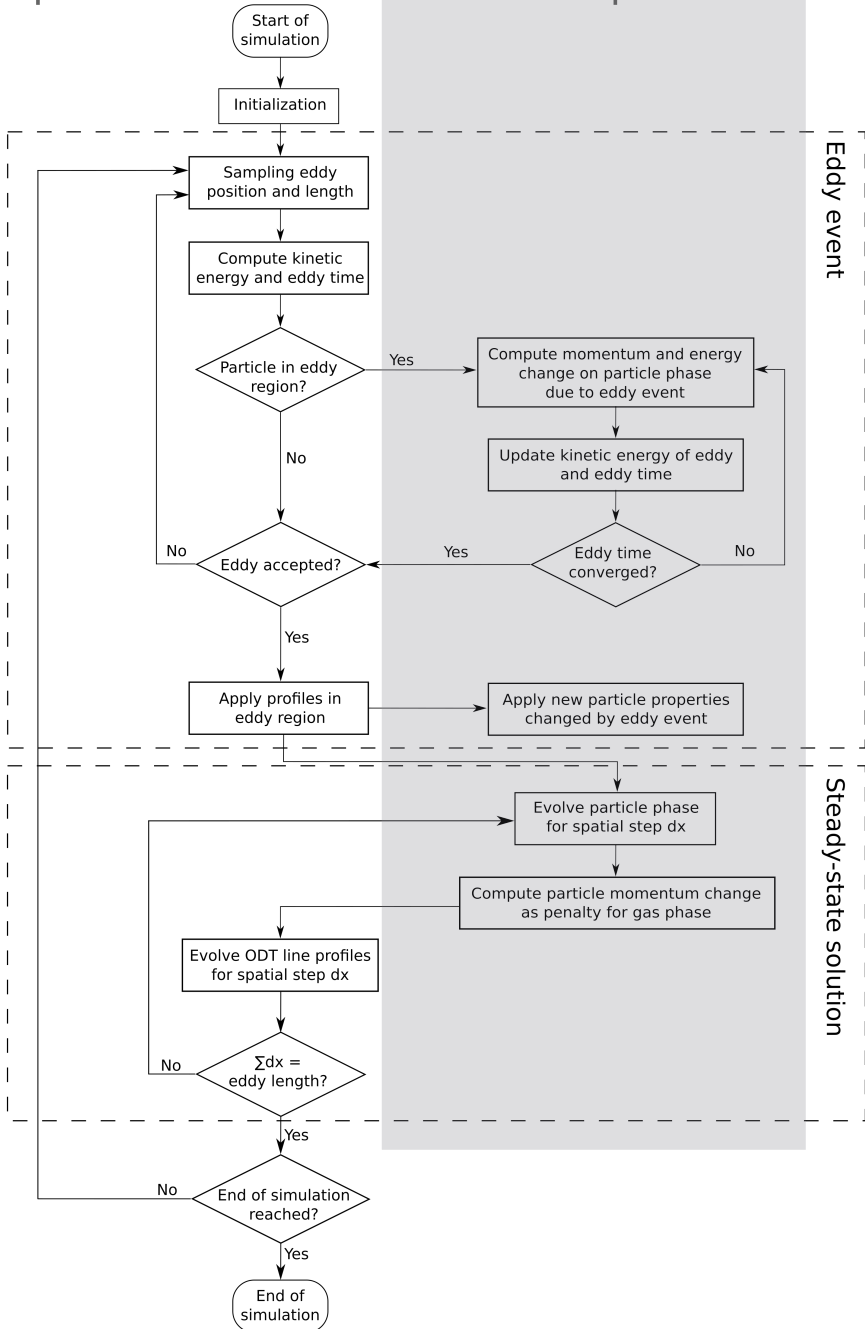


Figure 4.2: Flow chart of particle phase implementation for spatial ODT

# 5 Contribution to the Field

## 5.1 Paper I

*"Numerical study of stochastic particle dispersion using One-Dimensional-Turbulence"*

The first required step for this thesis was to implement the particle model into the ODT 2.0 framework and modify it towards for the cylindrical coordinate system and an evolution in spatial dimension. Using the newly-developed spatial-cylindrical ODT promised an improvement of predicting the carrier gas-phase and a better comparison with spatial experimental results. In this paper the first validation of the new model was published. It is investigating the radial dispersion and axial velocity decay of a hexadecane droplets in a jet configuration with a nozzle diameter of 7mm and Reynolds numbers ranging from 10000 to 30000. The ODT predicted data is compared with experiments of Kennedy and Moody [12] for a broad range of different Stokes numbers. The presented results show good agreement with the experimental data, reproducing the results of Sun et al. [25] without needing to transform the temporal coordinate.

## 5.2 Paper II

*"Numerical studies of turbulent particle-laden jets using spatial approach of one-dimensional turbulence"*

As we successfully validated the particle tracking in the previous paper the next step was to extend the model for a momentum transfer from the particle back to the gas phase, i.e. a two-way coupling approach. Therefore, we introduced a source term for the diffusive advancement equation and a new kernel formulation enabling to exchange momentum and energy from and towards the particle phase. To validate this extension, simulations were run for a particle-laden turbulent round jet with solid loadings 0, 0.5 and 1 and particle diameter  $25\mu\text{m}$  and  $70\mu\text{m}$  and compared to experimental data from Budilarto [3]. It could be shown that the model was capable of capturing turbulence modulation of particles in a turbulent round jet.



## 6 Future work

The overall objective of the present ongoing work is to provide data of turbulence-droplet interaction for the filtered scales of Large eddy simulations (LES). The initial phase of implementing the Lagrangian particle tracking model into the ODT framework was successfully completed. The next steps towards the overall goal will be investigation of the mechanisms of droplet interaction with turbulent shear flows.

LES, as the name says, transport large scales and filters out the small ones. The effects of these smaller scales is covered by subgrid-models, which are very sensitive to their parameters. To develop an alternative, which should be less depended on user-defined parameters, it is important to understand the filter process. Often this is done by applying a low pass filter to the Navier-Stokes equations. Therefore, the grid resolution is not required to be as fine as the ones of DNS grids. If we now look into two neighboring cells we will often find two different velocity vectors. The flow between these two vectors can be seen as a shear flow. These shear flow can be highly turbulent and influence passing droplets or vice versa. It is important to find the governing mechanisms for these phenomena and the depending parameters. The final goal is to use the chosen parameters and take out data from a data base fed with statistical ODT results and give the information back to the LES grid cells. To reach this goal intensive studies of turbulence-droplet interaction in shear flows are required.



# References

- [1] Ashurst, W. T., Kerstein, A. R., 2005. One-dimensional turbulence: Variable density formulation and application to mixing layers. *Phys. Fluids* 17, 1-26.
- [2] Balachandar, S., Eaton, J.K., 2010. Turbulent dispersed multiphase flow. *Rev. Fluid Mech.* 42, 111-133.
- [3] Budilarto, S. G., 2003. An experimental study on effects of fluid aerodynamics and particle size distribution in particle laden jet flows. PhD thesis, Purdue Univeristy, USA.
- [4] Bradshaw, P., Woods, W.A., 1971. An introduction to turbulence and its measurement. In *Thermodynamics and Fluid Mechanics Series*.
- [5] Clift, R., Grace, J. R. and Weber, M. E., 1978. Bubbles, drops and particle. Academic Press, New York.
- [6] Du, C., 2017. Studies of Diesel sprays under non-reacting and reacting conditions. PhD thesis, Chalmers University of Technology, Sweden.
- [7] U.S. Energy Information Administration, 2017. International energy outlook 2017. Report No. DOE/EIA-0484(2017).
- [8] Elghobashi, S, 1994. On predicting particle-laden turbulent flows. *Applied Scientific Research* 52, 309–329.
- [9] Geiss, S., Dreizler, A., Stojanovic, Z., Chrigui, M., Sadiki, A. and Janicka, J., 2004. Investigation of turbulence modification in a non-reactive two-phase flow. *Experiments in Fluids* 36 (2), 344-354.
- [10] Hewson, J. C., Kerstein, A. R., 2001. Stochastic simulation of transport and chemical kinetics in turbulent CO/H<sub>2</sub>/N<sub>2</sub> flames. *Combustion Theory and Modelling* 5, 669 - 697.
- [11] International Energy Agency, 2009. Transport, Energy and CO<sub>2</sub>. IEA Publication, France.
- [12] Kennedy, I.M, Moody, M.H.,1998. Particle dispersion in a turbulent round jet. *Experimental Thermal and Fluid Science* 18, 11–26.
- [13] Kerstein, A. R., 1999. One-dimensional turbulence: model formulation and application to homogeneous turbulence, shear flows, and buoyant stratified flows. *Journal of Fluid Mechanics* 392, 277-334.
- [14] Kerstein, A. R., 2013. Hierarchical parcel-swapping representation of turbulent mixing. *Journal of Statistical Physics* 153, 142 - 161.
- [15] Landahl, M.T., Mollo-Christensen, E., 1992. *Turbulence and Random Processes in Fluid Mechanics* (2nd ed.). Cambridge University Press. p. 10.
- [16] Lignell, D. O., Kerstein, A. R., Sun G. and Monson, E. I., 2013. Mesh adaption for efficient multiscale implementation of one-dimensional turbulence. *Theoretical and Computational Fluid Dynamics* 27(3-4), 273-295.
- [17] Maxey, M., Riley, J., 1983. Equation of motion for a small rigid sphere in nonuniform flow. *Physics of Fluids* 26, 883.

- [18] Paschereit, C.O., 2013. Turbulenz und Strömungskontrolle. Lecture slides, TU Berlin, Germany.
- [19] Poelma, C., 2004. Experiments in particle-laden turbulence. PhD thesis, TU Delft, Netherlands.
- [20] Pope, S. B., 2000. Turbulent Flows. Cambridge University Press, New York.
- [21] Schiller, L., Naumann, A.Z., 1933. Über die grundlegenden Berechnungen bei der Schwerkraftaufbereitung. Zeitschrift des Verein Deutscher Ingenieure 77, 318-320.
- [22] Schmidt, J. R., Wendt, J. O. L., Kerstein, A. R., 2004. Prediction of particle laden turbulent channel flow using the one-dimensional turbulence. Proceedings of IUTAM Symposium on Computational Approaches to Disperse Multiphase Flow.
- [23] Schmidt, J. R., Wendt, J. O. L., Kerstein, A. R., 2009. Non-equilibrium wall deposition of inertial particles in turbulent flow. Journal of Statistical Physics 37, 233-257.
- [24] Schreck, S. and Kleis, S., 1993. Modification of grid-generated turbulence by solid particles. Journal of Fluid Mechanics 249, 665-688.
- [25] Sun, G., Hewson, J. C., Lignell, D. O., 2016. Evaluation of Stochastic Particle Dispersion Modeling in Turbulent Round Jets. International Journal of Multiphase flow 89, 108-122.
- [26] Tchen, C., 1947. Mean Value and Correlation Problems connected with the Motion of Small Particles suspended in a turbulent fluid. PhD thesis, TU Delft, Netherlands.